

Studies in Hydrodynamic Thrust Bearings. I. Theory Considering Thermal and Elastic Distortions

C. L. Robinson and A. Cameron

Phil. Trans. R. Soc. Lond. A 1975 **278**, 351-366
doi: 10.1098/rsta.1975.0029

Email alerting service

Receive free email alerts when new articles cite this article - sign up in the box at the top right-hand corner of the article or click [here](#)

To subscribe to *Phil. Trans. R. Soc. Lond. A* go to: <http://rsta.royalsocietypublishing.org/subscriptions>

Phil. Trans. R. Soc. Lond. A. **278**, 351–366 (1975) [351]

Printed in Great Britain

STUDIES IN HYDRODYNAMIC THRUST BEARINGS

I. THEORY CONSIDERING THERMAL AND ELASTIC DISTORTIONS

By C. L. ROBINSON AND A. CAMERON

*Lubrication Laboratory, Department of Mechanical Engineering,
Imperial College of Science and Technology, London S.W. 7*

(Communicated by H. Ford, F.R.S. – Received 23 April 1974)

CONTENTS

	PAGE
NOMENCLATURE	352
INTRODUCTION	352
PREVIOUS WORK	353
HYDRODYNAMIC THEORY	353
ESTIMATION OF PAD SURFACE TEMPERATURES	357
COMPUTATION AND SOLUTION OF THE REYNOLDS AND ENERGY EQUATIONS	357
DISTORTION THEORY	359
Pressure bending	359
Thermal bending	361
Thermal bending of the pad	362
Thermal bending of the collar	362
Direct compression	363
Direct thermal expansion	364
SIMULTANEOUS SOLUTION OF ALL THE GOVERNING EQUATIONS	364
CONCLUSIONS	366
REFERENCES	366

The distortions of a thrust pad and its runner are analysed by solving the biharmonic equation of plate flexure by both elastic and thermal causes. The temperature and pressures are obtained from the simultaneous solution of the Reynolds and energy equations. The major simplification is the assumption of constant temperature through the *thickness* of the oil film, though it varies in both the other directions. The equations are set up and their reduction to a form suitable for computing is described. Four modes of distortion are considered, pressure and thermal bending, direct compression and direct thermal expansion.

NOMENCLATURE

d	displacement towards pad of its rotational centre from its geometric centre	T	lubricant film temperature
D	plate factor = $Et^3/[12(1-\nu^2)]$	T_b	pad back temperature
E	Young modulus	T_m	measured temperature
h	film thickness	T_v	tangential collar velocity
h_0	minimum film thickness	U	collar velocity in the x direction
J	mechanical equivalent of heat	V	collar velocity in the y direction
k	thermal conductivity of pad	x, y, z	cartesian coordinates
k_0	thermal conductivity of lubricant	α	linear thermal expansion coefficient
l	depth of thermocouples below pad surface	δ	radial grid increment
M	bending moment per unit run	ΔT	temperature difference
N_p	normal collar velocity	η	lubricant viscosity
p	lubricant film pressure	θ	angular polar coordinate
Q	shear force per unit run	ν	kinematic viscosity or Poisson ratio
\dot{Q}_z	heat flux to the bearing solids	ρ	lubricant density
r	radial polar coordinate	σ	lubricant specific heat
t	pad thickness	ϕ	angular grid increment
		ω	deflexion
		Ω	collar rotational speed

INTRODUCTION

Tilting pad bearings hold an interesting place in mechanical engineering. First the infinite slider bearing is the first bearing taught in undergraduate lectures on lubrication, because the geometry is said to be so simple. Secondly the tilting pad bearing designed, patented and analysed by Michell in 1905 almost certainly never worked by solely tilting as de Geurin & Hall showed experimentally in 1957. The bearing sat tight on its pivot and operated satisfactorily because it was sufficiently flexible to distort elastically and thermally. The elastic and especially thermal distortions are of over-riding importance for these bearings as the brief historical survey in the next section will make plain.

The full experimental analysis of these distortions has been gravely hindered by the lack of a means of measuring film thickness over the whole pad. The usual proximity meters, making use of capacity or inductance, suffer from several difficulties in operation and only measure a point at a time. Optical interferometry, which shows the whole field, overcomes many of these difficulties and has been used extensively in this laboratory for point and line contacts. In this work it has been extended to the study of thrust pads, giving the film shape over the whole pad instantaneously. It has a further advantage in being very sensitive. Each successive fringe indicates a change in film thickness of *ca.* $2\ \mu\text{m}$ which is ideal for this purpose.

Having obtained reliable film shapes, they can be analysed theoretically and the experimental and theoretical results compared.

The theory of thrust bearing distortion lubrication is considered in this part. In the next part the experimental technique for measuring film shape by a new type of test apparatus which uses interferometry is described. Results derived from the theory described here are then compared with those measured. In the final part, 'parallel surface' thrust bearings are considered both experimentally and theoretically.

PREVIOUS WORK

In the first forty years or so after the work of Michell (1905), attention was concentrated on mathematical techniques for the solution of finite bearings. Christopherson (1941) was the first to consider simultaneously the Reynolds and the energy equations to find the temperature and hence the viscosity variation of the oil. Experimentally Fogg (1946) found that a nominally parallel bearing would carry a load, a fact previously discovered by Beauchamp Tower (1891) but forgotten. Fogg suggested the action of the bearing was due to thermal expansion of the oil and so the effect was christened 'thermal wedge'. A number of people analysed this suggestion and showed that it was not 'powerful' enough to explain the observed load carried. Raimondi & Boyd (1955) pointed out the importance of curvature in nominally flat bearings. This had been suggested by Swift in the discussion to Fogg's paper, but unfortunately, it was printed with the discussion of another and was not appreciated.

After 1956 two lines of work are discerned. In the one the viscosity and density were allowed to vary with temperature in the plane of the bearing. The subsequent elastic and thermal distortions were then calculated. A number of papers were presented by Sternlicht and co-workers (1957–1962). The second approach considered the variation of viscosity through the thickness of the film. Variation of viscosity had been shown to account for the load carrying capacity of counter-rotating disks (Cameron 1951) and the term 'viscosity wedge' (Cameron 1958) was coined to describe it.

Dowson & Hudson (1963) showed that with correct boundary conditions the viscosity wedge seriously reduced the load capacity of the pivoted bearing and yielded negative pressures for the parallel bearing. The importance of thermal distortions were emphasized and shown to be more important than elastic deflexion. Hemingway (1965) studied their effect experimentally while Neal (1963) and Ettles & Cameron (1966) attempted simplified treatments. These papers were mainly without the aid of computers. Since their advent and common use the whole problem of variation of temperature throughout the system, causing changes in viscosity, density and film thickness can be treated.

The purpose of this paper is to analyse the distortions of the pad and thrust collar to give film shape by solving the biharmonic equation of plate flexure for both the elastic and thermal cases. The temperature and pressure distribution of the oil film are obtained from the simultaneous solution of the Reynolds and energy equations. The major simplification is the assumption of constant temperature through the thickness of the oil film. This is regrettable but without it the problem would be completely intractable.

The results of the computations are then compared in parts II and III with film thickness variation measured over the whole pad using a technique based on optical interferometry.

HYDRODYNAMIC THEORY

The equations of hydrodynamic lubrication, the Reynolds and energy equations are derived in a number of standard textbooks (see, for example, Cameron (1966) and Pinkus & Sternlicht (1961)) where the relevant assumptions made are also listed.

By using the system of coordinates given in figure 1, the Reynolds equation can be written

$$\frac{1}{r} \frac{\partial}{\partial r} \left(\frac{r h^3}{\eta} \frac{\partial p}{\partial r} \right) + \frac{1}{r^2} \frac{\partial}{\partial \theta} \left(\frac{h^3}{\eta} \frac{\partial p}{\partial \theta} \right) = \frac{6}{r} \left[\frac{\partial}{\partial r} (h r N_v) + \frac{\partial}{\partial \theta} (h T_v) \right]. \quad (1)$$

The centre of rotation of the runner is not at the centre of the bearing pad sector but at a distance d nearer the pad, hence if Ω is the rotor speed, equation (1) may be transformed by putting

$$r' \sin \psi = d \sin \theta, \quad r' \cos \psi = r - d \cos \theta,$$

$$T_v = \Omega r' \cos \psi = \Omega(r - d \cos \theta), \quad N_v = -\Omega r' \sin \psi = -\Omega d \sin \theta,$$

and expanding the left hand side thus

$$\frac{h^2}{r\eta} \left(h + 3r \frac{\partial h}{\partial r} - \frac{rh}{\eta} \frac{\partial \eta}{\partial r} \right) \frac{\partial p}{\partial r} + \frac{h^3}{\eta} \frac{\partial^2 p}{\partial r^2} + \frac{h^2}{r^2 \eta} \left(3 \frac{\partial h}{\partial \theta} - \frac{h}{\eta} \frac{\partial \eta}{\partial \theta} \right) \frac{\partial p}{\partial \theta} + \frac{h^3}{r^2 \eta} \frac{\partial^2 p}{\partial \theta^2} = \frac{6\Omega}{r} \left[(r - d \cos \theta) \frac{\partial h}{\partial \theta} - rd \sin \theta \frac{\partial h}{\partial r} \right]. \quad (2)$$

The two dimensional energy equation in cartesian coordinates may be written

$$\begin{aligned} \left(\frac{\rho U h}{2} - \frac{h^3}{12\nu} \frac{\partial p}{\partial x} \right) \frac{\partial}{\partial x} (\sigma T) + \left(\frac{\rho V h}{2} - \frac{h^3}{12\nu} \frac{\partial p}{\partial y} \right) \frac{\partial}{\partial y} (\sigma T) - \left[\frac{\partial}{\partial x} \left(h k_0 \frac{\partial T}{\partial x} \right) + \frac{\partial}{\partial y} \left(h k_0 \frac{\partial T}{\partial y} \right) \right] + \dot{Q}_z \\ = \frac{1}{J} \left\{ \frac{\rho \nu}{h} (U^2 + V^2) + \frac{h^3}{12\rho \nu} \left[\left(\frac{\partial p}{\partial x} \right)^2 + \left(\frac{\partial p}{\partial y} \right)^2 \right] \right\}. \quad (3) \end{aligned}$$

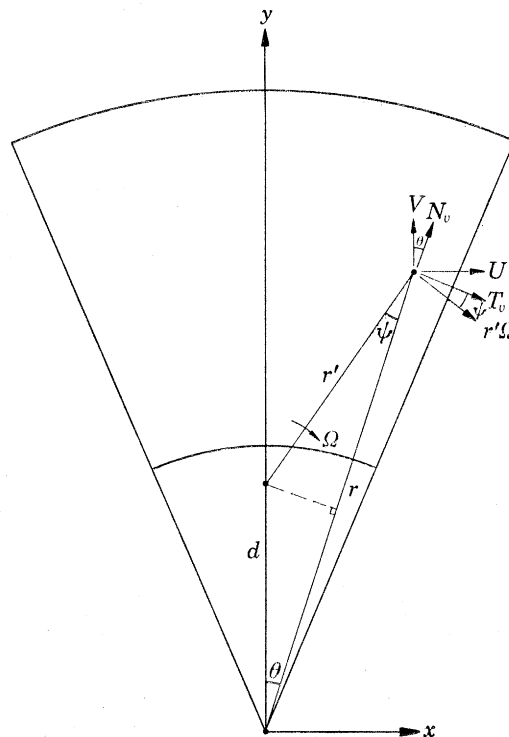


FIGURE 1. Coordinate system.

Now all previous work has ignored the conduction terms in equation (3). These terms are

$$\frac{\partial}{\partial x} \left(h k_0 \frac{\partial T}{\partial x} \right) + \frac{\partial}{\partial y} \left(h k_0 \frac{\partial T}{\partial y} \right), \quad (4)$$

which represents conduction within the fluid and \dot{Q}_z the heat flow per unit area to the bearing solids.

To obtain an expression for \dot{Q}_z two simplifying assumptions are made.

(1) The heat flow to the stationary pad is much larger than that to the runner. First

Christopherson (1957) showed that the temperature rise on the runner is small and secondly the runner is made of glass, a low thermal conductivity material.

(2) The temperature gradient in the pad, normal to its surface is linear. This is discussed later.

Hence

$$\dot{Q}_z = (k/t) (T - T_b), \quad (5)$$

where k is the thermal conductivity of the pad of thickness t and T and T_b are the temperatures of the front and back surfaces.

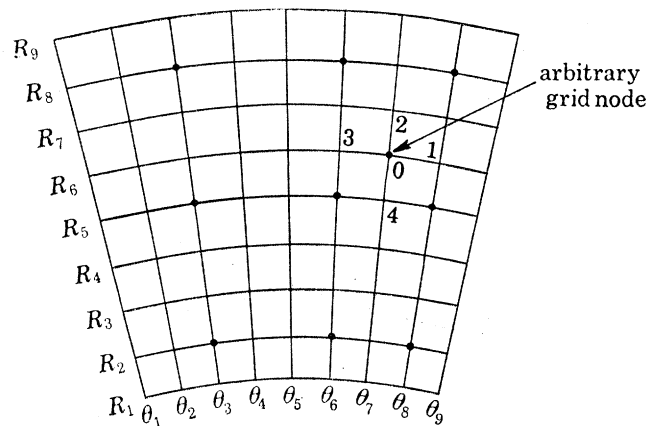


FIGURE 2. Computational grid.

An order of magnitude analysis for terms (4) and (5) shows that (5) is some 10^6 times larger than (4). Conduction within the fluid will, therefore, be neglected.

To put equation (3) into polar coordinates the standard transformations

$$\frac{\partial}{\partial x} = \sin \theta \frac{\partial}{\partial r} + \frac{\cos \theta}{r} \frac{\partial}{\partial \theta},$$

and

$$\frac{\partial}{\partial y} = \cos \theta \frac{\partial}{\partial r} - \frac{\sin \theta}{r} \frac{\partial}{\partial \theta},$$

are used.

Making these transformations, putting $\nu = \eta/\rho$, U and V in terms of r , θ and Ω and including equation (5) the energy equation becomes

$$\begin{aligned} \left[\frac{h\Omega}{2r} (r - d \cos \theta) - \frac{h^3}{12\eta r^2} \frac{\partial p}{\partial \theta} \right] \frac{\partial T}{\partial \theta} - \left(\frac{h\Omega d}{2} \sin \theta + \frac{h^3}{12\eta} \frac{\partial p}{\partial r} \right) \frac{\partial T}{\partial r} + \frac{k}{\sigma \rho t} (T - T_b) \\ = \frac{1}{\sigma \rho J} \left\{ \frac{h^3}{12\eta} \left[\left(\frac{\partial p}{\partial r} \right)^2 + \frac{1}{r^2} \left(\frac{\partial p}{\partial \theta} \right)^2 \right] + \frac{\eta}{h} r'^2 \Omega^2 \right\}. \end{aligned} \quad (6)$$

Referring to the 9×9 mode computational grid in figure 2 the derivatives in equations (2) and (6) can be replaced by finite difference expressions. For the Reynolds equation these are

$$\begin{aligned} \frac{\partial p}{\partial r} &= \frac{p_2 - p_4}{2\delta}, & \frac{\partial^2 p}{\partial r^2} &= \frac{p_2 - 2p_0 + p_4}{\delta^2}, \\ \frac{\partial p}{\partial \theta} &= \frac{p_1 - p_3}{2\phi}, & \frac{\partial^2 p}{\partial \theta^2} &= \frac{p_1 - 2p_0 + p_3}{\phi^2}. \end{aligned}$$

The Reynolds equation then reduces to

$$-2(A_2 + A_4)p_0 + (A_3 + A_4)p_1 + (A_1 + A_2)p_2 + (A_4 - A_3)p_3 + (A_2 - A_1)p_4 = B, \quad (7)$$

where

$$\left. \begin{aligned} A_1 &= \frac{h^2}{2\delta\eta r} \left(h + 3r \frac{\partial h}{\partial r} - \frac{rh}{\eta} \frac{\partial \eta}{\partial r} \right), & A_2 &= \frac{h^3}{\eta\delta^2}, \\ A_3 &= \frac{h^2}{2\phi\eta r^2} \left(3 \frac{\partial h}{\partial \theta} - \frac{h}{\eta} \frac{\partial \eta}{\partial \theta} \right), & A_4 &= \frac{h^3}{r^2\phi^2\eta}, \\ B &= \frac{6\Omega}{r} \left[(r - d \cos \theta) \frac{\partial h}{\partial \theta} - rd \sin \theta \frac{\partial h}{\partial r} \right]. \end{aligned} \right\} \quad (8)$$

The boundary conditions for this equation are that the pressure is zero everywhere on the pad boundary. For the 9×9 mesh shown in figure 2, 81 simultaneous equations in the pressures at each nodal point arise, 49 represent equation (7) and the remaining 32 are the boundary condition.

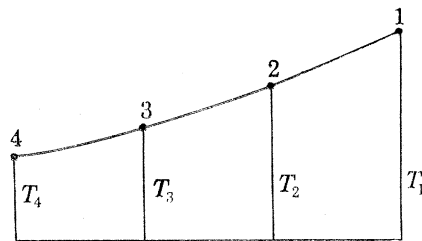


FIGURE 3. Extrapolation for the energy equation boundary conditions.

In a similar way the energy equation reduces to

$$X_0 T_0 + X_1 T_1 + X_2 T_2 - X_1 T_3 - X_2 T_4 = Z, \quad (9)$$

where

$$\left. \begin{aligned} X_0 &= \frac{k}{t\sigma\rho}, \\ X_1 &= \frac{h}{2r\phi} \left[\frac{\Omega}{2} (r - d \cos \theta) - \frac{h^3}{12\eta r} \frac{\partial \rho}{\partial \theta} \right], \\ X_2 &= -\frac{h}{2\delta} \left(\Omega d \sin \theta + \frac{h^3}{6\eta} \frac{\partial \rho}{\partial r} \right), \\ Z &= \frac{1}{\sigma\rho J} \left\{ \frac{h^3}{12\eta} \left[\left(\frac{\partial \rho}{\partial T} \right)^2 + \frac{1}{r^2} \left(\frac{\partial \rho}{\partial \theta} \right)^2 \right] + \frac{\eta}{h} r'^2 \Omega^2 \right\} + \frac{k}{\sigma\rho t} T_b \end{aligned} \right\} \quad (10)$$

and

$$r'^2 = r^2 + d^2 - 2rd \cos \theta.$$

The derivatives of ρ are, of course, expressed in their finite difference form as explained above.

The energy equation equates heat generated in the oil to the work done on it and hence only evaluates temperature *rise*. The temperature of the fluid at the 9 inlet boundary nodes must, therefore, be known.

For the two circumferential edges the most reasonable condition without losing generality was considered to be that of quadratic extrapolation. In figure 3, points 1, 2, 3 and 4 represent the temperature of four nodes on a radial grid line with point 1 on the circumferential boundary. The condition assumes that a parabola passes through all four points which results in the relation

$$T_1 - 3T_2 + 3T_3 - T_4 = 0. \quad (11)$$

STUDIES IN HYDRODYNAMIC THRUST BEARINGS. I

357

The same condition is applied to the outlet edge. Hence 81 simultaneous linear equations in the temperatures at the nodes, 49 representing the energy equation (9), 23 of type (11) and 9 of the type $T = T_{\text{inlet}}$ allow the temperature field to be calculated. In practice the inlet oil temperature was deduced from pad surface temperature measurements as described below.

ESTIMATION OF PAD SURFACE TEMPERATURES

As will be described in the experimental section the pad temperature T_m was measured at a number of points a distance l below its working surface. The temperature of the pad backing T_b was assumed equal to the temperature of the surrounding oil which was also measured. The surface temperature T is obtained assuming a linear temperature gradient through the pad thickness from the expression

$$T = (T_m t - T_b l) / (t - l). \quad (12)$$

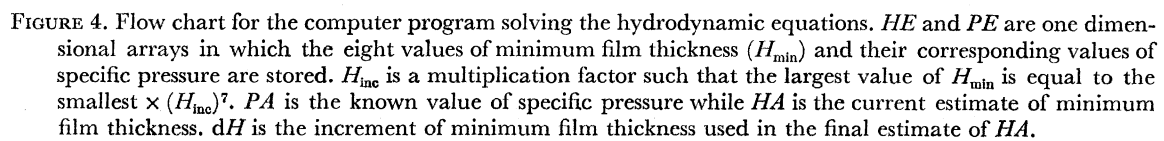
As l is much smaller than t this assumption cannot lead to serious error. For the tilting pad bearing the temperatures were measured at the 9 intersections of the radii $\theta_3, \theta_6, \theta_8$ and the circumferences R_2, R_5, R_8 , referring to figure 2. The temperatures at the remaining nodes were computed using quadratic interpolation and extrapolation thus giving a complete experimental temperature distribution. A similar procedure was used for the parallel surface bearing but was complicated by the fact that the measurement points did not coincide with the computational grid nodes.

COMPUTATION AND SOLUTION OF THE REYNOLDS AND ENERGY EQUATIONS

For the purpose of finding a simultaneous solution to the Reynolds and energy equations the following data are available: speed, load, bearing geometry and pad material and lubricant properties. Also from the experimental methods which are described in part II the film shape is known. From this information it is required to find the absolute film thickness and the film temperature and pressure distributions.

The individual solution to each equation was effected by solving the 81 simultaneous linear equations described by using a computer library subroutine based on the matrix pivotal method. The University of London CDC 6600 Computer and Fortran IV language were used throughout. Since the Reynolds and energy equations both contain viscosity terms their simultaneous solution cannot be obtained directly without prior knowledge of the viscosity distribution throughout the lubricant film. In the absence of these data, an iterative scheme must be employed and while this is quite feasible, and was originally written into the computer program, the convergence was found to be slow which resulted in the uneconomical use of computer time. As an estimation of the film temperature distribution was available from experimental measurements this was used to establish values of viscosity throughout the film. The temperature distribution calculated by the energy equation from these viscosity values was found to be in good agreement with that measured.

It is a relatively simple matter to calculate the bearing load by numerically integrating the pressure distribution corresponding to a known absolute film thickness. What is required here, however, is to calculate the minimum film thickness (h_0) from a known value of load, which is much more difficult and can only be accomplished by an iterative scheme; or more crudely, a trial and error method.



A series of solutions were first prepared for a range of eight values of h_0 between which the true value of h_0 was expected to be. (Values of 2 and 15 μm were used for the bearing analysed.) A 5×5 mesh solution was used for this purpose because while yielding less accurate results it reduced computing time tenfold. An estimate of the actual value of h_0 corresponding to the known bearing load was made by linear interpolation. A better estimate of h_0 was then obtained by finding more precise 9×9 mesh solutions for two values of minimum film thickness, one slightly greater and the other slightly less than the first estimate, and again by using linear interpolation. This estimate was further refined using the same procedure. The final load found from integrating the pressure distribution was always found to equal that measured within an error of $\frac{1}{2}\%$. A flow chart for the computer program which solves the hydrodynamic problem by the methods described is shown in figure 4.

DISTORTION THEORY

In order to calculate the distorted shape of the oil film from the temperature and pressure distributions arising from the simultaneous solution of the hydrodynamic equations, four modes of distortion are considered. These are pressure bending, thermal bending, direct compression, and direct thermal expansion. Ettles & Cameron (1963) in a simplified analysis considered only pad distortions whereas those of both the pad and the collar are considered in this study.

Pressure bending

The pressure bending of the pad or the collar is governed by the biharmonic equation of plate flexure which is derived in Timoshenko & Woinowski-Krieger (1959), p. 283 and with reference to the coordinate system of figure 1 may be expressed

$$\nabla^2(\nabla^2\omega) = p/D, \quad (13)$$

where

$$\nabla^2 = \frac{\partial^2}{\partial r^2} + \frac{1}{r} \frac{\partial}{\partial r} + \frac{1}{r^2} \frac{\partial^2}{\partial \theta^2},$$

the Laplacian operator, and $D = Et^3/[12(1-\nu^2)]$, the plate factor. The various forces and moments per unit run acting in the circumferential and radial direction are

$$\text{bending moments: } M_r = -D \left[\frac{\partial^2 \omega}{\partial r^2} + \nu \left(\frac{1}{r} \frac{\partial \omega}{\partial r} + \frac{1}{r^2} \frac{\partial^2 \omega}{\partial \theta^2} \right) \right], \quad M_\theta = -D \left(\frac{1}{r} \frac{\partial \omega}{\partial r} + \frac{1}{r^2} \frac{\partial^2 \omega}{\partial \theta^2} + \nu \frac{\partial^2 \omega}{\partial r^2} \right), \quad (14)$$

$$\text{twisting moments: } M_{r\theta} = (1-\nu) \left(\frac{1}{r} \frac{\partial^2 \omega}{\partial r \partial \theta} - \frac{1}{r^2} \frac{\partial \omega}{\partial \theta} \right), \quad (15)$$

$$\text{shear forces: } \left. \begin{aligned} Q_r &= -D \frac{\partial}{\partial r} (\nabla^2 \omega), \\ Q_\theta &= -D \frac{1}{r} \frac{\partial}{\partial \theta} (\nabla^2 \omega), \end{aligned} \right\} \quad (16)$$

$$\text{edge reactions: } \left. \begin{aligned} V_r &= Q_r - \frac{1}{r} \frac{\partial}{\partial \theta} (M_{r\theta}), \\ V_\theta &= Q_\theta - \frac{\partial}{\partial r} (M_{r\theta}). \end{aligned} \right\} \quad (17)$$

The boundary conditions depend on whether the pad or the collar is being considered and the relevant edge conditions are tabulated below.

edge condition	circumferential boundary ($r = \text{const.}$)	radial boundary ($\theta = \text{const.}$)
clamped	$\omega = 0, \quad \partial\omega/\partial r = 0$	$\omega = 0, \quad \partial\omega/\partial\theta = 0$
simply supported	$\omega = 0, \quad M_r = 0$	$\omega = 0, \quad M_\theta = 0$
free	$V_r = 0, \quad M_r = 0$	$V_\theta = 0, \quad M_\theta = 0$

For pressure bending of the pad the whole boundary is free. Timoshenko & Woinowski-Krieger (1959, p. 85) explain that in the case of a totally free boundary the twisting moments at each corner must also be equated to zero. The final condition which must be applied to this particular problem is that the deflexion of points lying above the pad support must be zero.

The pressure bending of the thrust collar depends on the method of absorbing the pad bearing reaction. In most commercial applications the thrust is transmitted along the shaft. In this case, however, the reaction is taken by a hydrostatic bearing for which details are given in the experimental part II. Figure 5 shows the hydrostatic bearing recess in relation to the pad; and for simplicity the hydrodynamic pressure is considered to act over the shaded area. As the pressure bending deflexions were found to be a small proportion of the total deflexion the error incurred by this simplification was not considered to be significant. The boundary conditions for this case were taken as simply supported for the circumferential boundaries, and clamped for the radial boundaries. Obviously, only the deflexion over the shaded area in figure 5 will contribute to the shape of the oil film.

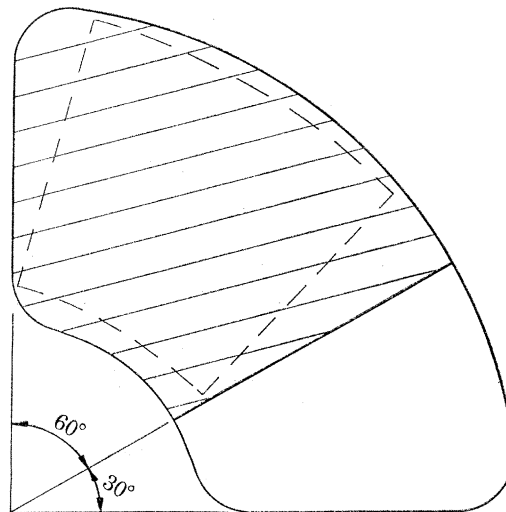


FIGURE 5. Hydrostatic bearing recess and thrust pad.

Since the biharmonic equation and the boundary conditions discussed contain only linear partial differential terms of deflexion in r and θ they will all reduce to a system of linear simultaneous equations when reduced to finite difference form. A 9×9 computational grid was again used and since the biharmonic equation and some boundary conditions contain third and fourth order derivatives of ω then two image points are required beyond the pad boundary to express these in finite difference form. The extended grid was then 13×13 . The complete finite difference forms of the biharmonic equation and the boundary conditions are given by Robinson (1971).

For the case of pressure bending of the pad the values of deflexion at 169 points are to be found and the following equations results

76	equations in $\nabla^4\omega = p/D$	(biharmonic equation)
5	$\omega = 0$	(deflexion at support point)
4	$M_{r\theta} = 0$	(corner boundary conditions)
18	$M_r = 0$	(circumferential boundary conditions)
18	$V_r = 0$	
18	$M_\theta = 0$	(radial boundary conditions)
18	$V_\theta = 0$	
12	$\omega = 0$	(unused image points)
169	total	

The number of equations equal the number of unknowns so the problem can be solved. A computer program has been written to compute this solution using the computer library subroutine already described. This program also solves the problem of thermal bending of the pad which is discussed later.

In order to check the program for pressure bending deflexion use was made of an analytical solution for the deflexion of a sector shape plate published by Deverall & Thorne (1951). They treated the case of a uniformly distributed pressure acting on the plate with radial edges simply supported and circumferential edges clamped. For a plate of 0.524 rad included angle, of thickness 6.36 mm and radial width equal in length to the mean circumferential arc under a pressure of 3.5 MPa the analytical solution gave a central deflexion of 1.65 μm . The finite difference computed solution for the same problem gave a value of 1.67 μm which allowed the method to be used with confidence.

Thermal bending

The frictional heat generated within the bearing oil film causes the thrust faces of the pad and the collar to thermally expand to a greater extent than their non-thrust faces and thermal bending results. In order to calculate the distortion due to this action some assumptions and simplifications are necessary even for a computer solution. These assumptions are listed and discussed.

- (1) Temperature varies linearly through the thickness of the pad and the collar. Neal (1963) demonstrated that the thermal gradient through these components was slightly non-linear but not to such an extent as to prevent this simplification being justified.
- (2) There is no difference between the temperature of the pad surface and that of the adjacent oil film as calculated by the energy equation. The major assumption here is that temperature is constant throughout the thickness of the oil film which was made to allow a tractable solution for the Reynolds and energy equations. Having once made this assumption it follows that it should be used again here.
- (3) The temperature of the collar thrust surface is constant in the direction of motion and equal to the average film temperature along an arc of constant radius. Christopherson (1957) showed this to be so and the analyses of Dowson & Hudson (1963) and Hunter & Zienkiewicz (1960) confirm it.
- (4) The temperature of the rear surface of the pad is equal to the bulk oil temperature in the bearing oil groove and the temperature of the non thrust surface of the collar is equal to that of oil at inlet to the housing. These are confirmed by measurements.

Thermal bending of the pad

The thermal bending of a plate of uniform thickness having an arbitrary temperature distribution over its front and rear faces and a linear thermal gradient through its thickness was treated by Goodier (1957). The analysis showed that a variable temperature difference ΔT across the plate thickness can be replaced by an equivalent mechanical loading. This takes the form of a distributed pressure q , where

$$q = \frac{D(1+\nu)\alpha}{t} \nabla^2(\Delta T), \quad (18)$$

with the symbols having their usual meaning and α is the coefficient of linear expansion of the plate material. There is also an edge loading on the boundary. This takes the form of an edge moment and an edge reaction in any arbitrary direction 'n' of M_n and V_n per unit run where

$$M_n = \frac{D(1+\nu)\alpha}{t} \Delta T \quad (19)$$

and

$$V_n = \frac{D(1+\nu)\alpha}{t} \frac{\partial}{\partial n}(\Delta T). \quad (20)$$

In polar coordinates this implies that the bending moments on circumferential and radial boundaries are

$$M_r = M_\theta = \frac{D(1+\nu)\alpha}{t} \Delta T, \quad (21)$$

and the edge reactions are

$$\left. \begin{aligned} V_r &= \frac{D(1+\nu)\alpha}{t} \frac{\partial}{\partial r}(\Delta T), \\ V_\theta &= \frac{D(1+\nu)\alpha}{t} \frac{1}{r} \frac{\partial}{\partial \theta}(\Delta T). \end{aligned} \right\} \quad (22)$$

Three further conditions are necessary to fix the distorted surface in space and these do not affect the equilibrium of the system. Two are chosen such that the deflexion at each edge of the pad support is zero and the third such that the deflexion at the centres of the two radial boundaries are equal. Having substituted the thermal loading with a distributed pressure and edge moments and reactions, the deflexions can be evaluated in exactly the same manner as previously described for pressure bending. The accuracy of the computer program was checked for thermal bending using the test case of a uniformly distributed temperature difference ΔT across the thickness of the pad for which the analytical solution is simply a spherical surface of curvature radius R , where

$$R = t/\alpha\Delta T. \quad (23)$$

The radius of curvature for the computer solution agreed with that calculated from equation (23) within 0.6 %.

Thermal bending of the collar

The temperature difference across the thickness of the collar is assumed constant in the direction of motion and it is, therefore, a function of radius only and the deflexion problem is reduced to one of axial symmetry. The deflexion of a circular disk under an axisymmetric load is treated by Timoshenko & Woinowski-Krieger (1959). If Q is the shear force per unit run at radius r the deflexion is given by the differential equation

$$\frac{d}{dr} \left[\frac{1}{r} \frac{d}{dr} \left(r \frac{d\omega}{dr} \right) \right] = \frac{Q}{D}. \quad (24)$$

STUDIES IN HYDRODYNAMIC THRUST BEARINGS. I 363

As discussed in the previous section the shear force corresponding to the thermal loading will be

$$Q = \frac{D(1+\nu)\alpha}{t} \frac{d}{dr}(\Delta T). \quad (25)$$

If ΔT is expressed as a cubic in r , i.e.

$$\Delta T = B_0 + B_1 r + B_2 r^2 + B_3 r^3, \quad (26)$$

equation (24) can be integrated to give

$$\omega = \frac{(1+\nu)\alpha}{t} \left(\frac{B_1}{9} r^3 + \frac{B_2}{16} r^4 + \frac{B_3}{25} r^5 + D_1 + D_2 \lg r + D_3 r^2 \right). \quad (27)$$

The three constants of integration D_1 , D_2 and D_3 may be found from the three boundary conditions which with reference to the previous section are

$$\omega = 0 \quad \text{and} \quad M_r = \frac{D(1+\nu)\alpha}{t} (\Delta T)_{r=a} \quad \text{at} \quad r = a \quad (28)$$

and

$$M_r = \frac{D(1+\nu)\alpha}{t} (\Delta T)_{r=b} \quad \text{at} \quad r = b,$$

where a and b are the inner and outer radii of the disk respectively, and the bending moment M_r is given by

$$M_r = D \left\{ \frac{d^2 \omega}{dr^2} + \frac{\nu}{r} \frac{d\omega}{dr} \right\}. \quad (29)$$

The values of ΔT at each radius in the finite difference grid were computed by taking the average of the nine calculated film temperatures. The arcs of constant radius for the pad computational grid do not quite coincide with those for the collar because the geometric centre of the pad model used and the centre of rotation do not coincide. However, the error due to this is small. A library subroutine which fits a polynomial of any order to a given set of data by Craut's reduction method is used to evaluate the four constants B_0 to B_3 . The computation of the integration constants from equations (28) and (29) is straightforward and from equation (27) the thermal bending deflexions are calculated.

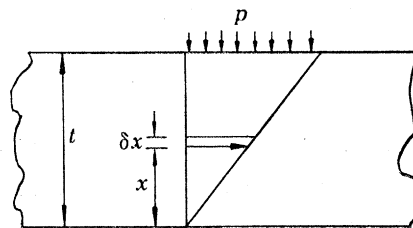


FIGURE 6. Pressure profile through the pad or collar.

Direct compression

The hydrodynamic pressure of the oil film will cause a direct compression of the pad and the collar. Assuming the compressive stress varies linearly through the thickness of each component the total movement of the working surface with reference to figure 6 will be

$$\omega = \int_0^t \frac{p x}{E t} dx = \frac{p t}{2 E}. \quad (30)$$

Summing the effect for both the pad and the collar the resulting change in film thickness where the film pressure is p will be

$$\omega = \frac{p}{2} \left(\frac{t_p}{E_p} + \frac{t_c}{E_c} \right), \quad (31)$$

where subscripts p and c refer to the pad and the collar.

Direct thermal expansion

Direct thermal expansion can be treated in a similar manner to direct compression. The temperature gradient through the thickness of the pad and the collar has already been assumed to be linear. Referring to figure 7 the thermal growth of an element of thickness δx a distance x from the non-thrust face will be

$$d\omega = \alpha \left[T_b + (T - T_b) \frac{x}{t} \right] dx. \quad (32)$$

The total growth of the thrust surface is, therefore

$$\omega = \alpha \int_0^t \left[T_b + (T - T_b) \frac{x}{t} \right] dx = \frac{1}{2} \alpha t (T + T_b). \quad (33)$$

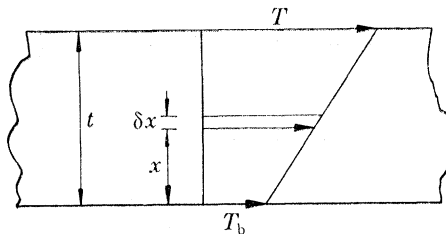


FIGURE 7. Temperature profile through the pad or collar.

Only the variation in thermal growth will affect the film shape and since T_b has been assumed constant for both pad and collar, it can be omitted. The full term for direct thermal expansion then becomes

$$\omega = -\frac{1}{2} (\alpha_p T_p t_p + \alpha_c T_c t_c). \quad (34)$$

The negative sign indicates that direct thermal expansion decreases film thickness whereas all other modes of deflexion increase it.

SIMULTANEOUS SOLUTION OF ALL THE GOVERNING EQUATIONS

A final computer program was written to solve both the hydrodynamic and elasticity equations simultaneously and satisfy their boundary conditions. The required input data are bearing geometry and material properties, lubricant properties, and the following operating parameters

- speed
- load
- pad inlet temperatures
- temperatures of the oil in the housing and at inlet.

A simplified flow chart is shown in figure 8. The hydrodynamic program already described is used to find solutions for temperature and pressure distributions and minimum film thickness.

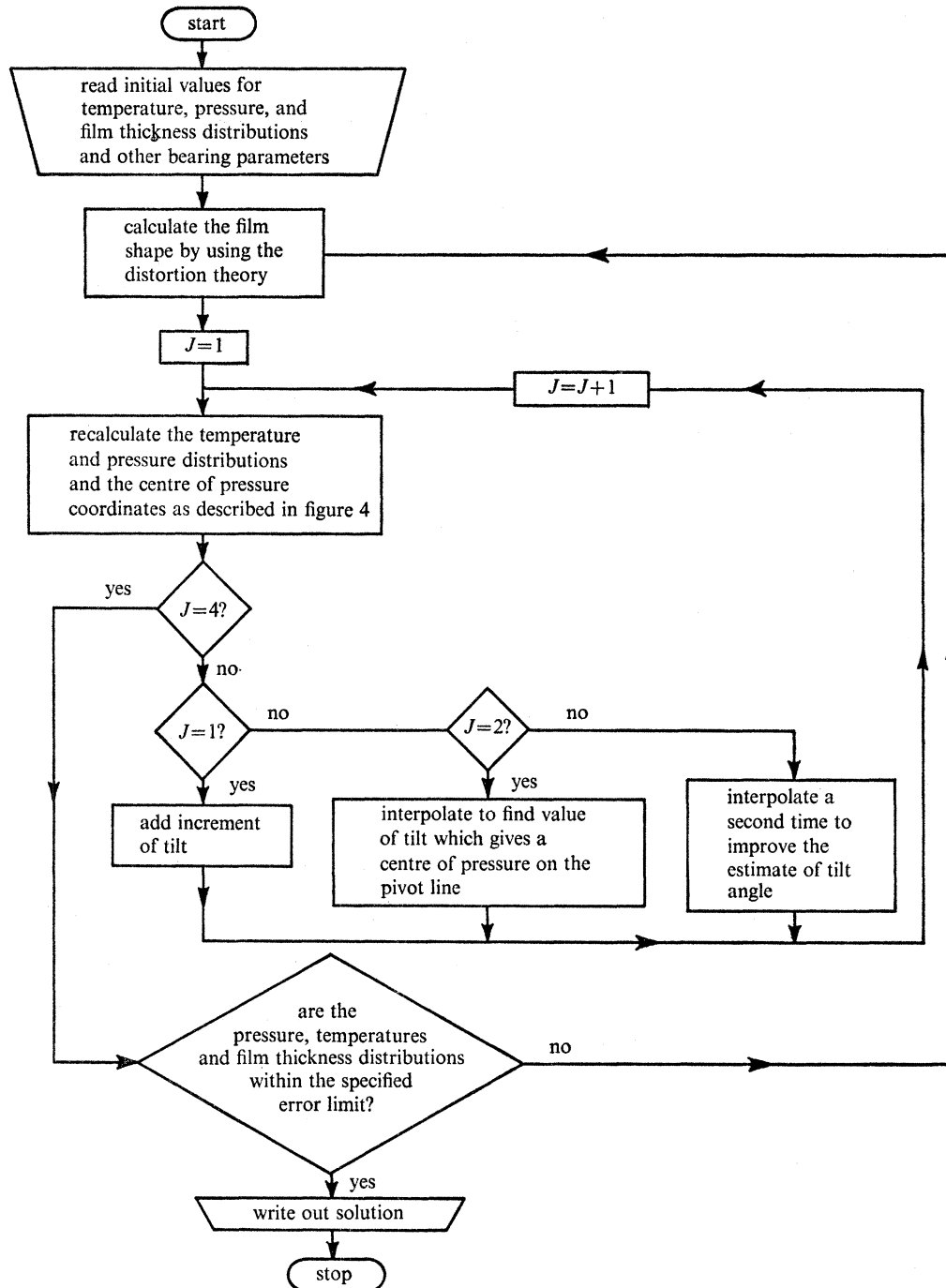


FIGURE 8. Flow chart for the full thrust bearing computer program.

Two further iteration loops are included. The first finds the correct angle of pad tilt using solutions from two assumed values and linear interpolation in a similar process to that used for finding minimum film thickness. The second iterates between solutions of the hydrodynamic equations and the distortion equations until successive solutions for temperature, pressure, and film thickness distribution agree within $\frac{1}{2}\%$ on a summation basis. The centre of pressure was always

found to lie within 0.03 % of the pad width from the axis of symmetry of the pad using this method. In practice three cycles of the outer iteration loop were required to reach a solution. Even so the programme took more than 400s of central processor time.

The derivation of all the equations and listings of the important parts of the computer programs are given by Robinson (1971).

CONCLUSIONS

This paper gives details of a computer solution for thrust bearings taking into account heat conduction as well as convection, and thermal and elastic distortions. The only major simplification has been to assume that temperature is constant across the thickness of the oil film, though varying in all other directions. A comparison of computed solutions with experimental measurement is described in the next two parts. Part II which follows, describes the interferometric apparatus and its application to a tilting pad bearing. Part III considers a parallel surface bearing.

REFERENCES

- Cameron, A. 1951 *J. Inst. Petrol.* **37**, 471.
 Cameron, A. 1958 *Trans A.S.L.E.* **1**, 254.
 Cameron, A. 1966 *Principles of lubrication*. London: Longmans.
 Christopherson, D. G. 1941 A new mathematical method for the solution of film lubrication problems. *Proc. I. Mech. Engrs*, **146**, 126.
 Christopherson, D. G. 1957 *Inst. Mech. Eng. Conf.* 1957, pp. 9–15.
 Deverall, L. I. & Thorne, C. J. 1951 Bending of thin ring-sector plates. *Trans. A.S.M.E. J. appl. Mech.* **18**, 359.
 Dowson, D. & Hudson, J. D. 1963 The thermo-hydrodynamic analysis of the infinite slider bearing. Part 1. The plane inclined slider bearing. *Lub. Wear. Conv. I. Mech. Engrs*, p. 31.
 Ettles, C. M. & Cameron, A. 1963 Thermal and elastic distortions in thrust bearings. *Lub. Wear. Conv. I. Mech. Engrs*, p. 57.
 Ettles, C. M. & Cameron, A. 1966 *Lub. Wear. Conv. I. Mech. Engrs*.
 Fogg, A. 1946 Fluid film lubrication of parallel thrust surfaces. *Proc. I. Mech. Engrs*, **155**, 49.
 Goodier, J. N. 1957 Thermal stress and deformation. *Trans A.S.M.E. J. appl. Mech.* **79**, 467.
 de Guerin, D. & Hall, L. F. 1957 Some characteristics of conventional tilting pad thrust bearings. *Lub. Wear. Conf. Proc. I. Mech. Engrs*, p. 142.
 Hemingway, E. W. 1965 The measurement of film thickness in thrust bearings and the deflected shape of 'parallel' surface thrust pads. *Proc. Inst. Mech. Engrs*, **180**, pt. 1, no. 44.
 Hunter, W. B. & Zeinkeiwicz, O. C. 1960 Effect of temperature variations across lubricant films in the theory of hydrodynamic lubrication. *J. mech. engng sci.* **2**, 52.
 Michell, A. G. M. 1905 The lubrication of plane surfaces. *Z. Mat. Phys.* **52**, 123.
 Neal, P. B. 1963 Film lubrication of plane faced thrust pads. *Lub. Wear. Conv. I. Mech. Engrs*, p. 49.
 Pinkus, O. & Sternlicht, B. 1961 *Theory of hydrodynamic lubrication*. New York: McGraw-Hill.
 Raimondi, A. A. & Boyd, J. 1955 The influence of surface profile on the load capacity of thrust bearings with centrally pivoted pads. *Trans A.S.M.E.* **77**, 321.
 Robinson, C. L. 1971 Thermal and elastic distortions in thrust bearings. Ph.D. Thesis, Univ. of London.
 Sternlicht, B. 1957 Energy and Reynolds consideration in thrust bearing analysis. *Lub. Wear. Conf. I. Mech. Engrs*, p. 28.
 Sternlicht, B. & Maginnis, F. J. 1957 Application of digital computers to bearing design. *Trans A.S.M.E.* **79**, 1483.
 Sternlicht, B., Ried, J. C. & Arwas, E. B. 1961 Performance of elastic, centrally pivoted thrust bearing pads. *Trans A.S.M.E. J. Basic Engng*, **83**, 169.
 Sternlicht, B., Carter, G. K. & Arwas, E. B. 1961 Adiabatic analysis of elastic, centrally pivoted thrust bearing pads. *Trans A.S.M.E. J. appl. Mech.* **28**, 179.
 Timoshenko, S. & Woinowski-Krieger, S. 1959 *Theory of plates and shells*. New York: McGraw-Hill.
 Tower, B. 1891 4th report on friction measurements. *Proc. Inst. Mech. Engrs*, pp. 11–40.